

Evaluation of neutron energy spectrum effects and RPV thru-wall attenuation based on molecular dynamics cascade simulations

R.E. Stoller ^{a,*}

^a *Metals and Ceramics Division, Oak Ridge National Laboratory, PO Box 2008, Oak Ridge, TN 37831-6376, USA*

Accepted 16 September 1999

Abstract

Displacement cascade formation in iron has been investigated by the method of molecular dynamics (MD) for cascade energies up to 40 keV. The results of these simulations have been used in the SPECOMP code to obtain effective, energy-dependent cross sections for two measures of primary damage production: (1) the number of surviving point defects expressed as a fraction of the those predicted by the standard secondary displacement model by Norgett et al., 1975 [M.J. Norgett, M.T. Robinson, and I.M. Torrens, Nucl. Eng. Des. 33, (1975) 50–54] and (2) the fraction of the surviving interstitials contained in clusters that formed during the cascade event. The primary knock-on atom (PKA) spectra for iron obtained from the SPECTER code have been used to weight these MD-based damage production cross sections in order to obtain spectrally-averaged values for several locations in commercial fission reactors and test reactors. An evaluation of these results indicates that neutron energy spectrum differences between the various environments do not lead to significant differences between the average primary damage formation parameters. In particular, spectrum-averaged defect production cross sections obtained for PWR and BWR neutron spectra were not significantly different. A representative application of the new defect production cross sections is provided by examining how they vary as a function of depth into the reactor pressure vessel wall. A slight difference was noted between the damage attenuation in a PWR vessel and a BWR vessel. This observation could be explained by a subtle difference in the energy dependence of the neutron spectra. Overall, the simulations indicate that spectrum-averaged defect production cross sections do not vary much among the various environments in light-water moderated fission reactors. As such, the results support the use of atomic displacements per atom (dpa) as a damage correlation parameter and provide guidance for choosing the primary damage source term in kinetic embrittlement models. © 2000 Elsevier Science S.A. All rights reserved.

1. Introduction

Radiation-induced embrittlement in reactor pressure vessel (RPV) steels has traditionally been correlated with exposure parameters such as the

* Tel.: +1-423-576-788; fax: +1-423-574-0641.
E-mail address: rkn@ornl.gov (R.E. Stoller)

neutron fluence above 1 MeV or atomic displacements per atom (dpa) (IAEA, 1975; Stoller and Odette, 1992; ASTM, E693, 521). One advantage of dpa over fast fluence is that it explicitly accounts for atomic displacements produced by the entire neutron energy spectrum. Therefore, it provides improved correlation of data obtained from irradiation facilities with different neutron energy spectra. Differences in neutron energy spectra are manifested as differences in the energy spectra of the primary knock-on atoms (PKA) that are produced in elastic collisions with these neutrons. Low energy PKA, such as those produced by thermal neutrons, are somewhat more efficient at net defect production than are high-energy PKA. This suggests that these displacements should be more heavily weighted in dosimetry. Conversely, the lower energy PKA produce fewer point defect clusters that can promote the formation of extended defects responsible for mechanical property changes.

The issue of PKA energy effects can be addressed through the use of displacement cascade simulations using the method of molecular dynamics (MD). Although MD simulations can provide a detailed picture of the formation and evolution of displacement cascades, they impose a substantial computational burden. However, recent advances in computing equipment permit the simulation of high energy displacement events involving more than one-million atoms (Stoller et al., 1996; Stoller, 1996a,b); the results presented below will encompass MD cascade simulation

energies from near the displacement threshold to as high as 40 keV. The computing time with the molecular dynamics (MOLDY) code is almost linearly proportional to the number of atoms in the simulation and higher energy events require a larger atom block as listed in Table 1. Two to three weeks of cpu time is required to complete the highest energy 40 keV cascade simulations with 1 024 000 atoms for 15 ps on a modern high-speed workstation.

Two parameters have been extracted from the MD simulations: the number of point defects that remain after the displacement event is completed and the fraction of the surviving interstitials that are contained in clusters. For the purpose of comparison with standard dosimetry, these values have been normalized to the number of atomic displacements calculated with the secondary displacement model by Norgett et al. (1975). The energy dependence of the two MD defect parameters was used to evaluate the effects of neutron energy spectrum. Simple, energy-dependent functional fits to the MD results were obtained and the SPECOMP code (Greenwood, 1989) was used to compute effective cross sections for point defect survival and point defect clustering. PKA spectra for iron obtained from SPECTER (Greenwood and Smither, 1985) were then used to weight these effective cross sections in order to calculate spectrum-averaged values for various neutron irradiation environments. These include several locations through the wall of RPVs of representative commercial pressurized and boiling water reactors

Table 1
Typical MD cascade parameters and required atom block sizes

Neutron energy (MeV)	Average PKA energy (keV)	Corresponding E_{MD} (keV)	NRT displacements	Atoms in simulation
0.0034	0.116	0.1	1	3456
0.0058	0.236	0.2	2	6750
0.014	0.605	0.5	5	6750
0.036	1.24	1.0	10	54 000
0.074	2.54	2.0	20	54 000
0.19	6.60	5.0	50	128 000
0.40	13.7	10.0	100	250 000
0.83	28.8	20.0	200	250 000
1.8	61.3	40.0	400	1 024 000

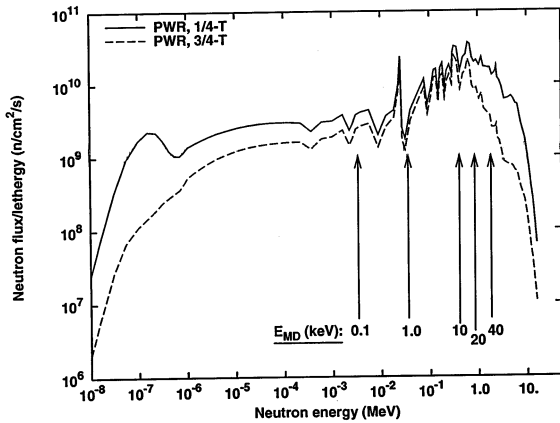


Fig. 1. Representative PWR neutron spectra at the 1/4-T and 3/4-T RPV locations and the corresponding average cascade energy.

(PWR and BWR) and positions in both water and sodium-cooled materials test reactors.

2. MD cascade simulations

The molecular dynamics code, MOLDY, and the interatomic potential for iron that was used are described in detail in Finnis and Sinclair (1984, 1986), Finnis (1988), Calder and Bacon (1993). Additional details on the results obtained by this method can be found in Phythian et al. (1995), Stoller et al. (1996), Stoller (1996a,b). Briefly described, the process of conducting a cascade simulation requires two steps. First, a block of atoms of the desired size is thermally equilibrated, this process permits the lattice thermal vibrations (phonon waves) to be established for the simulated temperature, and typically requires a simulation: equivalent to approximately 10 ps. This atom block can be saved and used as the starting point for several subsequent cascade simulations. Then, the cascade simulations are initiated by giving one of the atoms a defined amount of kinetic energy, E_{MD} , in a specified direction. This atom is equivalent to the PKA following a collision with a neutron. Statistical variability can be introduced by either further equilibration of the starting block or by choosing either a different primary knock-on atom or PKA

direction. Typically, at least six different cascades are required to obtain statistically representative average parameters at any one cascade energy and temperature.

The MOLDY code describes only elastic collisions between atoms; it does not account for energy loss mechanisms such as electronic excitation and ionization. Thus, the initial energy E_{MD} given to the simulated MD PKA is analogous to the damage energy (T_{dam}) in the NRT model (Norgett et al., 1975). Using the values of E_{MD} in Table 1 the corresponding E_{PKA} and the NRT defects in iron have been calculated using the procedure described in Norgett et al., (1975) with the recommended 40 eV displacement threshold (ASTM, E521). These values are also listed in Table 1. Note that the difference between the MD simulation, or damage energy and the PKA energy increases as the PKA energy increases.

The cascade simulations are continued until in-cascade recombination of vacancies and interstitials is complete and the atom block has returned to near thermal equilibrium. The required simulation time varies from about 5 ps for the low-energy cascades to 15–20 ps for the 40 keV cascades at 100 K. The range of neutron energies covered by these simulations is also listed in Table 1 and illustrated in Fig. 1. The neutron spectra obtained at the 1/4-T and 3/4-T RPV positions for a typical PWR are shown and the corresponding MD simulation energies are indicated.

Two parameters are of primary interest to this work: the number of point defects that survive after in-cascade recombination is complete and the fraction of the surviving interstitials contained in clusters rather than as isolated defects. The former is important because it is only the surviving point defects that can contribute to radiation-induced microstructural evolution. The latter is significant because these small clusters provide nuclei for the growth of larger defects which can give rise to mechanical property changes. The formation of these small clusters directly within the cascade means that the extended defects can evolve more quickly than if the clusters could only be formed by the much slower process of classical nucleation. For purposes of this work, interstitials were considered clustered if they were within the

nearest-neighbor lattice distance of another interstitial. The size distribution of the interstitial clusters produced is a function of the cascade energy (Phythian et al., 1995) and the interstitial clustering fraction is calculated by summing that distribution.

The surviving MD defects can be conveniently described as a fraction of the NRT displacements (Norgett et al., 1975) and the number of clustered interstitials as a fraction of the surviving MD defects. The energy dependence of the surviving defect fraction (η) and the interstitial clustering fraction (f_{icl}) from the MD simulations is shown

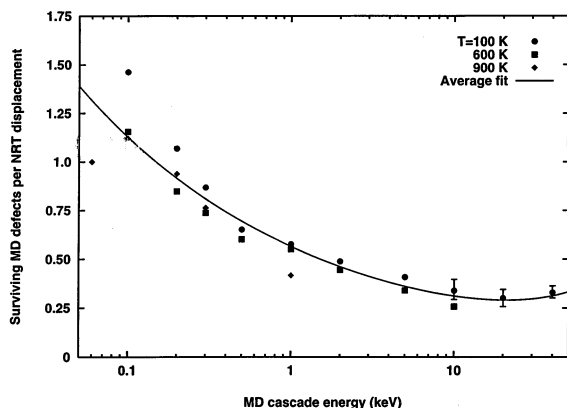


Fig. 2. Average MD point defect survival fraction as a function of cascade energy; results of MD simulations at 100, 600 and 900 K.

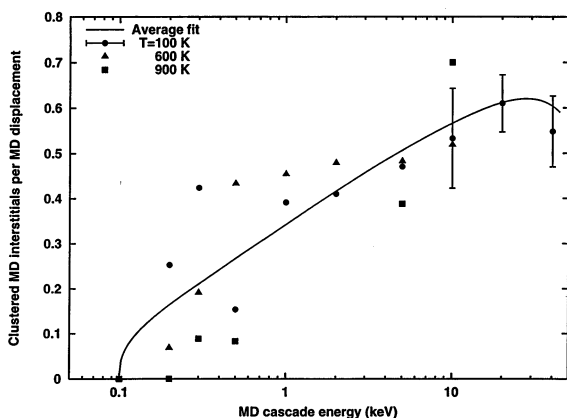


Fig. 3. Average in-cascade interstitial clustering fraction as a function of cascade energy; results of MD simulations at 100, 600 and 900 K.

in Figs. 2 and 3, respectively. Since the MD results did not exhibit a strong dependence on irradiation temperature, all of the results obtained at 100, 600, and 900 K are shown (Phythian et al., 1995; Stoller et al., 1996; Stoller, 1996a,b). The line drawn through the data in each figure is a nonlinear least-squares fit to the data using the following functions:

$$\eta = 0.5608 \cdot E_{MD}^{-0.3029} + 3.227 \times 10^{-3} \cdot E_{MD} \quad (1)$$

$$f_{icl} = [0.097 \cdot \ln(E_{MD} + 0.9)]^{0.3859} - 7 \times 10^{-6} \cdot E_{MD}^{2.5} \quad (2)$$

where E_{MD} is in keV.

In both Eqs. (1) and (2), the first term in the function dominates the energy dependence up to about 20 keV. The second term accounts for the effect of subcascade formation at the highest energies (Stoller et al., 1996; Stoller, 1996a). Mathematically, this term is responsible for the minimum in the defect survival curve and the maximum in the interstitial clustering curve at about 20 keV. This change in the energy dependence occurs because subcascade formation makes a high single energy cascade appear to be the equivalent of several lower energy cascades. Thus, the defect survival fraction is slightly higher and the interstitial clustering fraction slightly lower at 40 than at 20 keV. The phenomenon of subcascade formation is illustrated in Fig. 4, in which typical 10, 20, and 40 keV cascades are shown.

The increase in the defect survival fraction between 20 and 40 keV is slight, but it appears to be statistically significant from the magnitude of the standard deviations that are shown as error bars in Fig. 2. Since the standard deviations on the average interstitial clustering fractions are much larger, the significance of the maximum shown in Fig. 3 is less clear. No cascades with energies higher than 40 keV have been completed at this time. However, based on the degree of subcascade formation observed in the 40 keV cascade simulations, it appears unlikely that η and f_{icl} will change significantly at higher cascade energies. Therefore, the values calculated from Eqs. (1) and (2) for 40 keV were applied for all the higher energy PKA in the SPECOMP and SPECTER calculations.

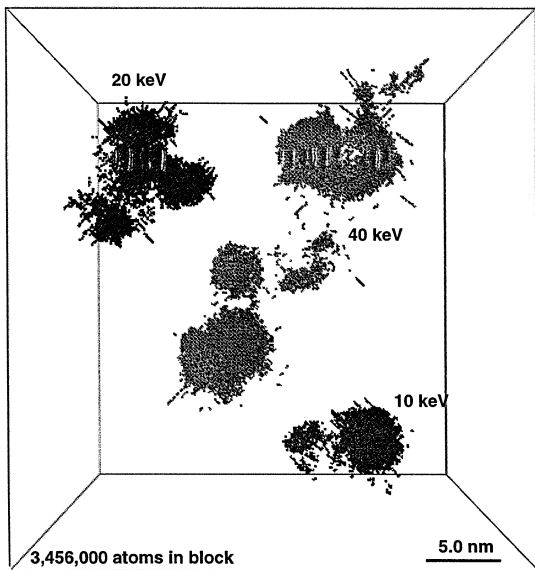


Fig. 4. Illustration of increasing subcascade formation in iron at 100 K as the MD cascade energy increases from 10 to 40 keV.

3. Defect production calculations using SPECOMP and SPECTER

Energy-dependent defect production cross sections for surviving MD defects and clustered interstitials and spectrum-averaged values for several irradiation environments were generated by modifying the SPECOMP (Greenwood, 1989) and SPECTER (Greenwood and Smither, 1985) computer codes. SPECOMP normally calculates displacement cross sections for compounds using the primary knock-on atomic recoil energy distributions contained in a 100-neutron-energy by 100-recoil-energy grid for each of 40 different elements. For the present defect and clustered interstitial calculations, these new functions were used as a factor multiplying the standard displacement cross section equations as a function of the damage energy, T_{dam} . SPECOMP thus produced surviving defect and clustered interstitial cross sections on a 100 point neutron energy grid.

The SPECTER computer code contains libraries of calculated cross sections for displacements, gas production and total energy distribution, as well as atomic recoil energy distributions for more

than 40 elements and various compounds. For a given neutron energy spectrum and irradiation time, the code can be used to calculate the net radiation damage effects, as listed above. In the present case, the SPECOMP calculations for the surviving defect and clustered interstitial cross sections were added to the SPECTER libraries. SPECTER runs for various neutron spectra thereby producing spectrum-averaged values for the point defect and interstitial clustering fractions.

4. Results and discussion

The primary results of these calculations are summarized in Fig. 5. The PKA-spectrum-averaged defect survival fraction is shown in Fig. 5a and the interstitial clustering fraction in Fig. 5b. In both cases, the effective production cross sec-

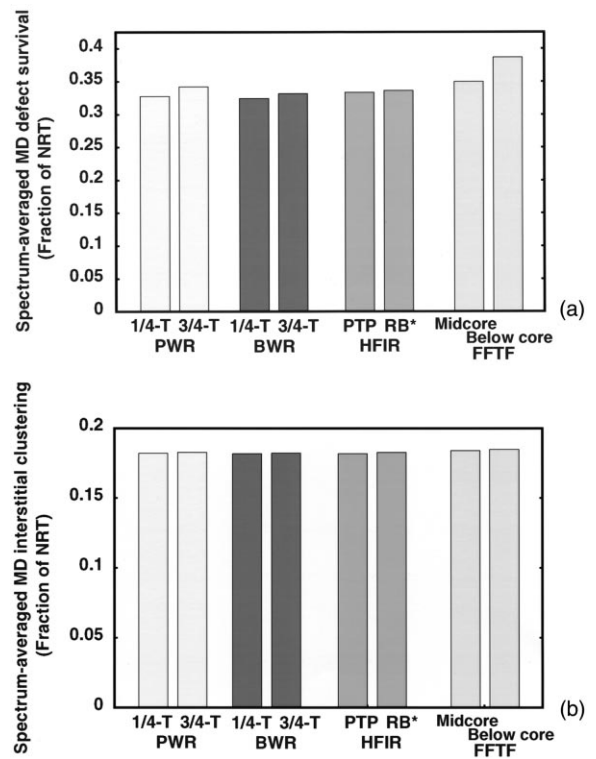


Fig. 5. Comparison of spectrally-averaged damage production cross sections (per NRT dpa) for various irradiation environments; defect survival ratio is shown in (a) and the interstitial clustering fraction is shown in (b).

tion has been divided by the NRT dpa cross section. Values are shown for the 1/4-T and 3/4-T RPV positions from representative PWR and BWR neutron spectra. Four additional irradiation sites are also shown. These are: positions located in the peripheral target position (PTP) and removable beryllium reflector (RB*) of the high flux isotope reactor (HFIR) at ORNL and the mid-core and below-core (BC) positions in the fast flux test facility (FFTF) at the US DOE Hanford Reservation.

Including the HFIR and FFTF positions pro-

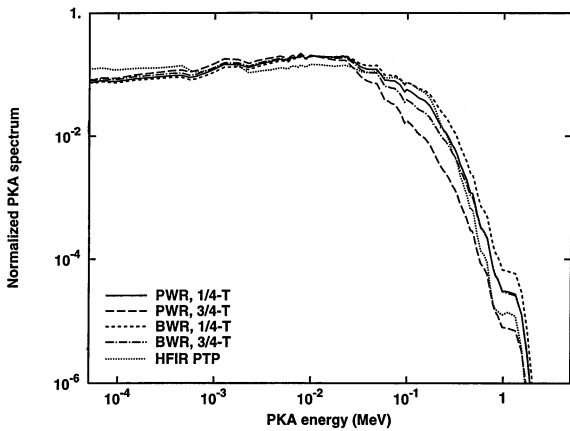


Fig. 6. Normalized iron PKA spectra for PWR and BWR 1/4-T and 3/4-T positions and the HFIR PTP position.

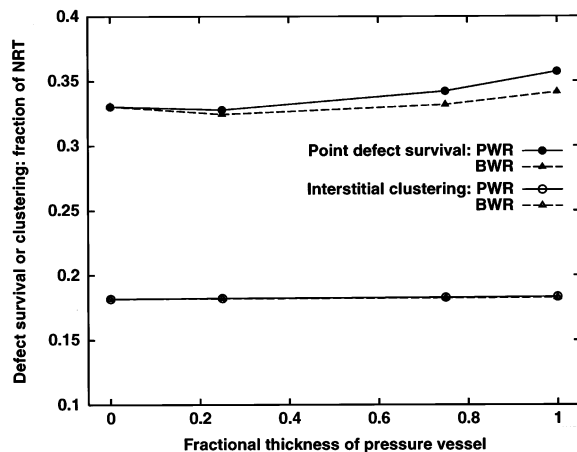


Fig. 7. Variation of spectrally-averaged damage production cross sections (per NRT dpa) through the RPV for PWR and BWR.

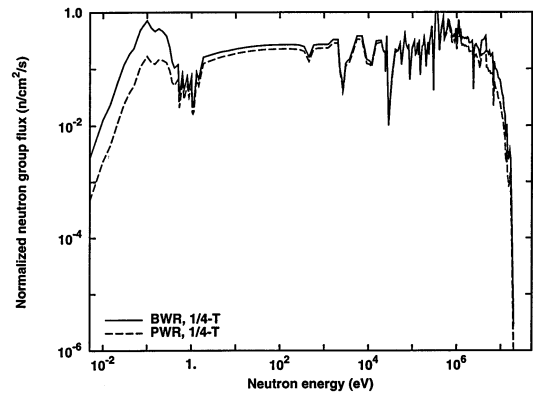


Fig. 8. Comparison of normalized neutron spectra for PWR and BWR at the 1/4-T RPV location. Note that the BWR has both higher relative thermal and fast fluxes.

vides a broad comparison of both hard and soft neutron spectra. The former is a very high-flux (up to $\sim 10^{15}$ n cm⁻²), water-moderated test reactor and the latter is a liquid metal (Na) cooled fast reactor. In spite of the differences between the neutron energy spectra, only relatively small differences are observed in the two spectrum-averaged damage cross sections. This is consistent with the normalized iron PKA spectra shown in Fig. 6. In the region where the PKA probability is highest, i.e. for PKA energies between 1 keV and 0.1 MeV, the spectra are quite similar.

A slight difference between the PWR and BWR spectra can be seen in the way the spectra change as a function of thickness through the pressure vessel. This is illustrated in Fig. 7, where the spectrum-averaged defect production cross sections are shown for four positions: the last water node point before the RPV, the 1/4 and 3/4 RPV locations and the first node point in the cavity beyond the RPV. The values for the two reactor types are most similar at the pressure vessel wall and diverge somewhat at greater depths. The reason for this modest divergence is a subtle difference in the neutron energy spectra and the way in which neutron attenuation occurs. The BWR spectrum is generally considered to be softer than the PWR and would be expected to give a higher defect survival fraction based on the results shown in Fig. 2. However, the average PKA energy at the 1/4-T and deeper positions is actually some-

what higher for the BWR. This can be rationalized by a comparison of the 1/4-T neutron spectra in Fig. 8, where the energy-dependent fluxes are normalized using their respective peak values. The BWR spectrum shows both a higher relative thermal flux and a higher relative fast flux than the PWR spectrum. Since most of the displacements are generated by the higher energy neutrons, the effective average energy for the BWR spectrum is greater than that of the PWR.

5. Summary

Although it is not yet possible to simulate the highest energy displacement cascades generated in the materials used in fission reactors, the analysis of MD cascade simulations in iron for energies up to 40 keV provides considerable insight. The primary damage parameters derived from the MD results exhibit a strong dependence on cascade energy up to 10 keV; however, this dependence is diminished and slightly reversed between 20 and 40 keV. This reversal is due to the formation of well defined subcascades in this energy region. Analysis of the cascades indicates that little further change should occur at higher energies, which suggests that the results reported here should be relevant to an evaluation of neutron energy spectrum effects.

Notably, the spectrum-averaged defect production cross sections calculated for several fission reactor neutron spectra were all quite similar. This included locations within the pressure vessels of commercial PWRs and BWRs, as well as locations in light water and liquid metal cooled materials test reactors. As a result of the degree of similarity between the cross sections being so high, it appears unlikely that spectral differences will significantly influence comparisons of PWR and BWR data. In addition, since the effective damage production cross sections could be described by similar fractions of the NRT displacements, these results support the use of dpa as a damage correlation parameter. Finally, the spectrum-averaged defect production cross sections obtained from the MD results can be used to

guide the selection of appropriate radiation damage source terms in the kinetic models used to investigate radiation-induced microstructural evolution and embrittlement.

Acknowledgements

The assistance of Dr L.R. Greenwood from the Materials and Chemistry Division of the Pacific Northwest National Laboratory in carrying out the SPECTER and SPECOMP calculations is gratefully acknowledged. Research sponsored by the Office of Nuclear Regulatory Research, US Nuclear Regulatory Commission under inter-agency agreement DOE 1886-8199-8L with the US Department of Energy and by the Division of Materials Sciences, US Department of Energy under contract DE-AC05-96OR22464 with Lockheed Martin Energy Research Corp.

References

- ASTM E521, 1999, Standard practice for neutron radiation damage simulation by charged-particle irradiation, Annual Book of ASTM Standards, vol. 12.02, American Society of Testing and Materials, Philadelphia.
- ASTM E693, 1999, Standard practice for characterizing neutron exposures in iron and low alloy steels in terms of displacements per atom (dpa), Annual Book of ASTM Standards, vol. 12.02, American Society of Testing and Materials, Philadelphia.
- Calder, A.F., Bacon, D.J., 1993. *J. Nucl. Mater.* 207, 25–45.
- Finnis, M.W., 1988. MOLDY6-A: Molecular Dynamics Program for Simulation of Pure Metals; AERE R-13182, UKAEA, Harwell Laboratory.
- Finnis, M.W., Sinclair, J.E., 1984. *Phil. Mag.* A50, 45–55.
- Finnis, M.W., Sinclair, J.E., 1986. Erratum. *Phil. Mag.* A53, 161.
- Greenwood, L.R., 1989. SPECOMP: Calculations of Radiation Damage in Compounds. In: Farrar, H., Lippincott, E.P. (Eds.), *Reactor dosimetry: methods, applications and standardization*; ASTM STP 1001. American Society of Testing and Materials, West Conshohocken, PA, pp. 598–602.
- Greenwood, L.R., Smither, R.K., January, 1985. SPECTER: Neutron Damage Calculations for Materials Irradiations; ANL/FPP/TM-197. Argonne National Laboratory, Argonne, IL. Recommendations of IAEA specialists meeting

- on radiation damage units in graphite and ferritic and austenitic steels. *Nucl. Eng. Des.* 33, (1975), 48.
- Norgett, M.J., Robinson, M.T., Torrens, I.M., 1975. *Nucl. Eng. Des.* 33, 50–54.
- Phythian, W.J., Stoller, R.E., Foreman, A.J.E., Calder, A.F., Bacon, D.J., 1995. *J. Nucl. Mater.* 223, 245–261.
- Stoller, R.E., 1996a. *J. Met.* 48, 23–27.
- Stoller, R.E., 1996b. *J. Nucl. Mater.* 233–237, 999–1003.
- Stoller, R.E., Odette, G.R., 1992. *J. Nucl. Mater.* 186, 203–205.
- Stoller, R.E., Odette, G.R., Wirth, B.D., 1996. Primary defect formation in bcc iron: presented at the International Workshop on defect production, accumulation, and materials performance in irradiation environments, Davos, Switzerland, October 2–8, 1996. Accepted for publication in *J. Nuclear Mater.* 251 (1997) 49–60.